# Hybrid Coupling of Laser Light sources to Silicon (Oxy)Nitride Based Waveguides

A.J.T de Krijger and H.H.P.Th. Bekman

TNO Physics and Electronics Laboratory, Oude Waalsdorperweg 63,
NL-2597 AK The Hague, The Netherlands

## ABSTRACT

An efficient method was developed to couple a diode laser to a high contrast waveguides. The laserdiodes were mounted with sub-micron precision using a thermocompression mounting technique. An AlGaAs ($\lambda = 850$ nm) laserdiode was coupled to a SiON based slab waveguide (efficiency $\eta = 25-30\%$) and to a $Si_3N_4$ based ridge waveguide (efficiency $\eta = 20\%$) on silicon. A start has been made with the determination of the lifetime of thermocompression mounted laserdiodes. AlGaAs ($\lambda = 850$ nm) lasers as well as AlGaInP ($\lambda = 675$ nm) lasers were tested. The first results indicate that lifetimes in the range 10-30 years are possible for CW operation at 30°C. The laser-waveguide coupling technique is demonstrated in a sensor platform.

**Keywords:** Integrated Optic, Sensor, Diode Laser, Glass Optical Waveguides, Thermocompression. Hybrids. Lifetime Studies, Laser-Waveguide Coupling, Reactive Ion Etching, Silicon (oxy)nitride

## 1. INTRODUCTION

Integrated optical components have the advantage of smallness and ruggedness. At the same time the smallness makes normal coupling to an active light source (laserdiode) very critical, especially when the laser is coupled to high contrast waveguides. High contrast waveguides are preferred because they allow for efficient coupling to the high contrast lasers, and they allow small bending radii and thus small device area. Hence one approach aims to integrate the laserdiode and the waveguide in the same material system. However there are many examples in which the components are preferably not made from the III-V semiconductor material from which the lasers are made but from other materials such as oxides, niobates, phosphates, arsenates or others. Often, these materials have some special optical properties which makes their use desirable, such as optical non-linearity, magneto-optical effects, piezo-optic effects and others. III-V materials also have many of these properties but the coefficients involved are usually rather small. Also interesting materials can be found in organic chemistry such as polymers which also may exhibit large optical non-linearity and high electro-optical coefficients. Hence it is obvious that some connection technology which directly connects III-V semiconductor lasers to other materials such as the examples mentioned, will be of high technical interest.

Many different glass optical waveguides can be deposited on silicon substrate. The natural oxide of the material is very suitable as an optical buffer layer since it is transparent over a very wide wavelength range. Silicon wafers are produced in vast quantities for the electronics industry, they combine an excellent (surface) quality and strength with a relatively low price. Since silicon is the mainstay of the modern micro-electronics industry, it provides the advantages of compatibility with conventional semiconductor technology and equipment. In addition silicon has the potential to integrate vast quantities of micro-electronics and also short-wavelength photodiodes with the optical circuit. Therefore connection of semiconductor lasers to substrates with silicon integrated circuits is attractive and directly leads to functional units in which e.g. the laser current source and power stabilization, as well as the photodiode and its preamplifier can directly be integrated with the lasers. Also the fast growing micro-machining technology on silicon can give extra momentum to the field of hybrid opto-electronics on silicon.

The development of innovative micro systems for sensor applications is widely recognized as being important for a modern and competitive economy. Clear market signs point to the demand for miniaturized sensor systems for a

Other author information: (Send correspondence to H.B.)
A.K.: Email: krijger@fel.tno.nl; Telephone: +31-70-324 0459; Fax: +31-70-328 0961;
H.B.: Email: bekman@fel.tno.nl: Telephone: +31-70-324 0444: Fax: +31-70-328 0961

**Table 1.** Summary of typical coupling efficiency as function of laser-waveguide mis-alignment

| Alignment | Size ($\mu$m) | Efficiency (%) |
|---|---|---|
| Ideal | - | 90 |
| Transversal displaced | 0.3 | 45 |
| Laser-wg distance | 1.0 | 45 |

large variety of markets like health care, safety and security, defense and process control. Obvious advantages for these systems include low weight, high reliability, low volume and power consumption. Silicon integrated optic micrc sensors can be used for the detection of (bio-)chemical substances as well as for measurement of physical quantities like distance, pressure or temperature.

The work presented in this paper is part of a joint project of the TNO Physics and Electronics Laboratory and the University of Twente on silicon integrated optic micro sensors.

## 2. HYBRID LASER-WAVEGUIDE COUPLING SCHEMES

Coupling of laserdiodes to high-contrast waveguides requires a very accurate alignment between laser and waveguide. In Tab.1 we summarize the typical influence of mis-alignment on coupling efficiency. The results indicates that we require sub-micron alignment and mounting. In the following paragraphs we review some of the methods found in literature and we end up with the method used in the laser-waveguide coupling experiments in the current paper.

### 2.1. Solder

Commercially available laserdiodes are normally soldered with indium or gold/tin eutectic solder on a copper or silicon submount. It is therefore natural to use similar soldering techniques for a hybrid laser-waveguide coupling. One can either pursue an active or a passive alignment process. The production costs of passive aligned laser-waveguide couplings is lower than active aligned couplings.

Disadvantages of the use of solder are related to the use of solder flux (disturbing the laser-waveguide coupling). and to the fact that sudden failure of laser operation can occur due to solder-bond failure.[1,2] Among the metallurgical deteriorations observed were solder migration into the laser crystal due to current-induced local heating near the end mirror of the laser, indium whisker growth due to electromigration in indium solder, and tin whisker growth, when using gold-tin alloy as solder, due to strain relaxation.

#### 2.1.1. Active

In an active alignment scheme one first optimizes the laser-waveguide coupling after which the laser is soldered. Due to the flow of the solder the alignment is degraded. Yamada *et al.*[3] used Au-Sn solder and reached an alignment accuracy of $\pm 1$ $\mu$m.

#### 2.1.2. Passive

In passive-aligned soldering one makes use of alignment structures made in the substrate. The alignment structures are aligned with the waveguide using photolithography with sub-micron resolution. The laserdiode is pressed against the alignment structures after which the laserdiode is soldered. A disadvantage of this mounting technique is that the laserchips employed must be very similar. The position of the stripe relative to the side of the laserchip must be accurate to within 1 $\mu$m. Friedrich *et al.*[4] have made special laserdiode structures with self-aligned cleaving grooves. He finds a laser-waveguide alignment accuracy of $\pm 1$ $\mu$m.

A third laser-waveguide coupling technique uses the solder itself to achieve the alignment. During solder reflow a self-alignment takes place. This technique is used for flip-chip soldering and was first introduced by IBM.[5] The molten solder wets only the metal pads defined by lithography. If the metal pad and laser are mis-aligned than the surface tension of the molten solder will re-align them as the energy of the assembly is minimized. The typical alignment accuracy reported in literature is again $\pm 1$ $\mu$m.[6]

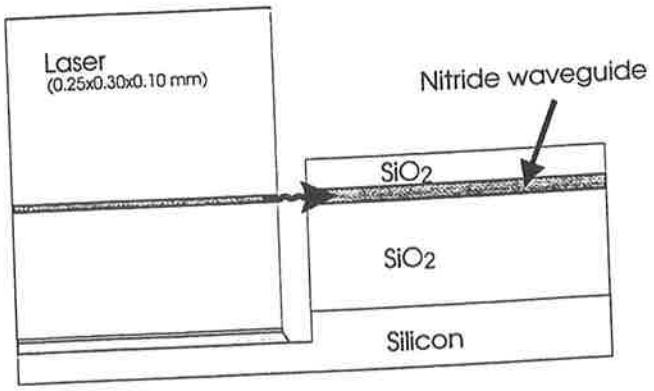


**Figure 1.** Schematic representation of laser-waveguide coupling

## 2.2. Glue

One could also glue a laser in front of a waveguide or glue a butt-end coupled laser with submount to the waveguide structure. The use of glue is more common for the coupling of fibers to waveguides.[7] Yamada *et al.* reported for such a coupling an accuracy of again $\pm 1$ $\mu$m. Reliability of the adhesive especially in high-humidity environments is an important issue.

We have undertaken a butt-end coupling technique of a laser on a sub-mount to a high-contrast slab waveguide with UV curing glue. The coupling efficiency could be rather high (50 %). The biggest problem which surfaced was the mechanical stability. The coupling efficiency varied strongly as function of temperature. The variation was caused by the expansion and shrinking of the glue beneath the laser submount.

## 2.3. Van der Waals adhesion

A very specialized but elegant coupling technique is named epitaxial lift-off. For a review of this technology and its applications see Demeester *et al.*.[8] In this scheme a GaAs laser is grown on a GaAs substrate with in between an AlAs lift-off or sacrificial layer. After fabrication of the laser the device structure layers above the AlAs are released from the GaAs substrate by using a selective AlAs etchant. The thin device structure film is than grafted on e.g. a silicon substrate in front of a waveguide. The film can be bonded to the new substrate via Van der Waals bonds. This technology is still strongly in the research stage. Problems with film stresses, bond integrity (contamination, smoothness) are topics of research.

The disadvantage of this technology is that one requires specially prepared laserdiodes which have an AlAs release layer incorporated in their structure. Furthermore the technology is thus far best developed for the GaAs material system. The residual stresses in the grafted laser film will accelerate laser degeneration. Advantages are related to the intimate contact between device film and substrate which is favorable for good thermal conduction. The device film bonded to a substrate can be thermally processed to high temperatures since no adhesives are involved.

## 2.4. Thermocompression

The laser-waveguide coupling used in the present study makes use of sub-micron alignment with a piezo-electric manipulator and thermocompression bonding. In thermocompression bonding no liquid materials are involved: the bond is created solely by material transport in the solid phase. The temperature during bonding is far below the melting temperature of the materials used. As a result the thickness of the bonding layers should remain constant during the process. Therefore the critical transversal alignment (0.1 $\mu$m)is achieved solely by tuning the metallization thickness, and the alignment achieved before bonding remains in theory also after bonding.

If two perfectly clean and flat metal surfaces would be brought into contact strong metal bonds will be created. In reality surfaces are never ideal. In this case strong metal-metal bonds can only be created when the thermocompression technique is employed. The process variables: temperature, pressure and time compensates the absence

of ideal surfaces. The yield strength of the bond can be as high as the strength of the individual materials. The strongest thermocompression bond is achieved between two identical materials (e.g. gold-gold).[9]

The thermocompression process can be divided into two stages.[10] In the first stage surface roughness will be reduced due to plastic deformation under the applied pressure. This process is instantaneous and it increases the contact area between the two metal layers. In the next stage the rest of the surface roughness will disappear as a result of the applied temperature and pressure due to lateral diffusion processes and creep. These process are strongly time dependent.

Because the metal layers remain in the solid phase during the whole process the transversal alignment of laser and waveguide is almost unaltered. A gold-gold thermocompression process is attractive. The advantages of gold are that the material is soft and that it does not oxidize. Nevertheless gold also has its specific problems one should be aware off. Gold surfaces get e.g. contaminated with organic substances. If gold surfaces are exposed to air for 6 months Jellison[11] found with Auger spectroscopy a layer of carbon of 2 nm. These organic films are stable to minimal 250°C[12] and disrupt the thermocompression process. A disadvantage of gold is that gold is not able to absorb this contamination. The solubility of carbon, oxygen and hydrogen in gold is very low. Enjyo *et al.*[13] concluded that some surface roughness was beneficial for a good thermocompression bond. He argued that the plastic deformation of the surface roughness breaks the contamination on the surface of the material.

The advantage of this coupling technique is that sub-micron alignment can be achieved. It is also versatile since almost any laserdiode can be used. A disadvantage of the technique is that it is active and that high bonding pressures are required which can be detrimental for the laserdiode lifetime.

## 3. EXPERIMENTAL

### 3.1. Method

In Fig.1 the schematic drawing of the laser-waveguide coupling which is used in the present study is given. In a waveguide structure an anisotropic well is etched. The bottom of the well is metallized. With a home-made manipulation setup the laser is actively positioned in front of the waveguide with sub-micron accuracy.' After the active alignment the laser is bonded to the substrate with thermocompression.

The top layer of the laserdiode metallization consists of gold. Therefore it was most natural to employ a gold-gold thermocompression process. The process is carried out under normal atmospheric conditions. Bonding under vacuum is however also frequently reported in literature. The vacuum partly cleans the surfaces by desorption processes. We rejected vacuum bonding for practical reasons. We use a process temperature of 250°C, a pressure of 180 bar and a bonding time of more than 10 minutes. The temperature of 250°C is well away of the melting temperature of gold (1064°C). In normal thermocompression practice the bonding temperature is set at a temperature around 70% of the melting temperature (which is around 663°C for gold). We have used only 250°C in order to protect the laser contact metallization integrity. As a result we had to use a relatively high bonding pressure. The yield strength of gold is 230 bar.[14] Normal thermocompression practice is to use a bonding pressure of 0.05 - 0.1 times the yield strength.

### 3.2. Laserdiodes

Two laserdiode families are used in the experiments. At first we started with 850 nm laserdiodes, since they are mass-produced, highly reliable (CD-laser application), and readily available. The laserdiodes were provided by the Opto-Electronic Center of Philips Research in bare chip form, with typical dimensions of 300 by 250 $\mu$m and a height of 100 $\mu$m. We want to use the new coupling technique in stand-alone micro-optic sensors. Therefore we also used visible laserdiodes ($\lambda$ = 675 nm) since transduction layers for chemical optical evanescent field sensors are more abundant in this wavelength region. These laserdiodes were also acquired from Philips. The exact location of the laser spot relative to the mounting surface on the epi-side is determined using the electron beam induced current (EBIC) mode of a scanning electron microscope. The values give in Tab.2 have an estimated accuracy of $\pm$0.1 $\mu$m.

**Table 2.** Typical characteristics Philips quantum-well laserdiodes

| Property | Type 1 | Type 2 |
|---|---|---|
| Wavelength | 675 nm | 850 nm |
| $I_{threshold}$ | 25 mA | 13 mA |
| Max. optical power | 13 mW ($I_f$ = 60 mA) | 20 mW ($I_f$ = 60 mA) |
| Far field angle $\parallel$ | 7° FWHM | 8 – 9° FWHM |
| Far field angle $\perp$ | 35° FWHM | 49° FWHM |
| Material system | GaInP/AlInP | AlGaAs/GaAs |
| Position laser spot | 3 $\mu$m | 2 $\mu$m |

### 3.3. Waveguide

The laser-waveguide coupling technique based on thermocompression precision mounting is not restricted to an unique laser or waveguide configuration. With regards to the optical waveguide the only requirement is that a nice straight well can be etched in the waveguide materials. This is not a trivial problem since a rather deep well of typically 3-4 $\mu$m has to be etched in a waveguide stack consisting of at least 2 (waveguide core and one type of buffer layer) and at most 4 different materials (waveguide core, two different buffer layers and substrate).

In previous reports on this laser-waveguide coupling we used a high-contrast $SiO_2/Al_2O_3/SiO_2$ waveguide.[15] In this paper we will describe the coupling to slab SiON based waveguides and to ridge $Si_3N_4$ based waveguides (both high-contrast). As buffer layers we used $SiO_2$.

Our starting material is thermally oxidized silicon. The thickness of the buffer oxide is typically 1-3 $\mu$m. On top of the oxide a SiON layer (n=1.79 @ 633 nm, thickness 310 nm) or $Si_3N_4$ layer (n=2.00 @ 633 nm. 338 nm thickness) was deposited with chemical vapor deposition (CVD) technique. The materials were optimized for low optical loss, uniformity of refractive index and uniformity of layer thickness.[16,17] Via lithography and wet etching using buffered hydrogen-fluoride straight waveguide structures were etched in the $Si_3N_4$ (in SiON no ridge waveguides were defined). The etch depth was only a 6 nm and the width of the waveguide was 4 $\mu$m. After waveguide definition a cladding $SiO_2$ layer (n=1.468 @ 633 nm, thickness 300 nm ($Si_3N_4$), 396 nm (SiON)) layer was deposited also with CVD technique.

## 4. LASER-WAVEGUIDE COUPLING

### 4.1. Masking and well etching

By using a sputtered chromium mask layer (thickness typical 0.3 $\mu$m) we have etched both the $SiO_2$ and the $Si_3N_4$ or SiON layers by a RIE etch processes. The bottom of the etched well was smooth. In case of $Si_3N_4$ the etch step used for the definition of the ridge waveguides showed up in the bottom of the well. But since this step was only 6 nm it was not detrimental for the laser-waveguide coupling. The side wall of the etched well was a little rough. probably due to the grain structure of the chromium metal mask. The $Si_3N_4$ as well as the SiON guiding layer was underetched by around 300 nm for a well depth of 3 to 4 $\mu$m. This underetch negatively influences the coupling efficiency since the laser-waveguide distance increases, it can further introduce harmful reflections back into the laser. The steepness of the etched well (of about 10%), which is present for both waveguide systems, further increases the laser-waveguide distance by an extra 0.3 $\mu$m. The total laser-waveguide distance will be more than 0.6 $\mu$m due to practical limitations.

### 4.2. Metallization

After the well etching the bottom of the well had to be metallized. A multi-layer metallization was deposited with e-beam evaporation technique. The top layer was gold, since we used a gold-gold thermocompression process. During metallization the side-wall of the well with waveguide had to be protected. We could either use the shadow effect which is present in the low-pressure evaporation process or we could use lift-off techniques with photo resist. Both techniques work satisfactory.

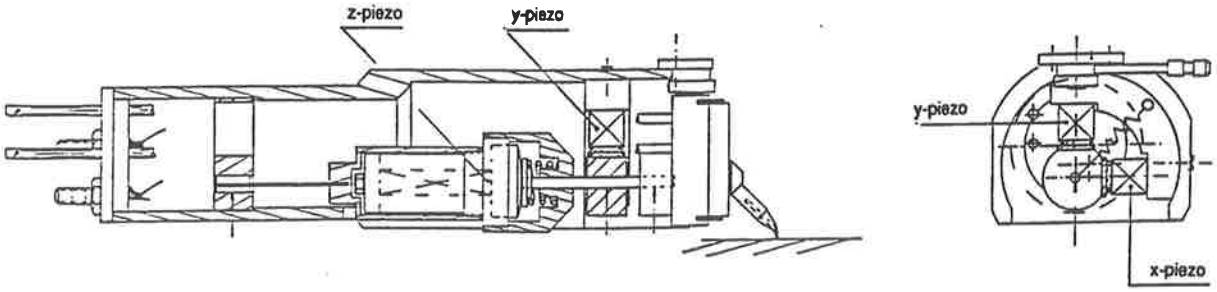


**Figure 2.** Piezo-electric laser positioner

### 4.3. Laser positioning and mounting

The lasers were positioned and mounted using a home-made manipulation set-up. The basic system consists of a mounting table (with vacuum chuck and heater) on top of electro-mechanically driven translation (x,y) and rotation stages and a piezo-electrically driven laser manipulator (see Fig.2). The substrates with waveguides are roughly positioned with the translation/rotation stages relative to a laserdiode chip attached by vacuum to the hypodermic needle of the laser manipulator. The laser at the end of the needle can be fine positioned with three piezo crystals (x,y,z) to optimize laser-waveguide alignment. The transversal and lateral alignment of the laser (x, y piezo) is controlled by piezos with an extension of 5 $\mu$m at 1000 V. The laser-waveguide distance (z piezo) is controlled by a piezo which extends 20 $\mu$ at 1000 V. The cross-talk between the different directions was better than 1:100. This was essential for good alignment. The pressure needed in the thermocompression process is applied via a membrane above the needle which is driven pneumatically. The mounting procedure is monitored by two zoom microscopes (20-150x) equipped with CCD video cameras. The microscopes are mounted under 90° and 45° relative to the mounting plane. As the CCD cameras are sensitive in the near IR region the 850 nm laser beam when coupled in the waveguide can be traced due to light scattering in the waveguide. The fine alignment was monitored by a photodiode at the waveguide end.

### 4.4. Experimental results

#### 4.4.1. Coupling

850 nm lasers were coupled to the SiON slab waveguides (length 12 mm). Typical coupling efficiencies were in the range 25-30%. These values were corrected for a 10% reflection loss at the waveguide end. The current-power curves of the bare laser, of the laser after optimum alignment but before bonding, and of the same laser after bonding are depicted in Fig.3 (left).

The coupling experiments to $Si_3N_4$ ridge waveguides were more difficult. This was caused by the used ridge waveguide structure. The waveguides were defined by an etch step of only 6 nm. Only with the 45° microscope system under critical illumination conditions the waveguides can be found after some exercises. It is essential that the front side of the laser is exactly parallel with the etched well in order to minimize laser-waveguide distance. We have coupled lasers to various ridges on one and the same substrate. The coupling efficiency is typically 20%. This value has been corrected for 10% attenuation in the 10 mm long ridge and 10% reflection loss at the waveguide end. The current-power plots of a typical coupling are depicted in Fig.3 (right). We deduced from measurements that 60% of the total power is coupled in the ridge. When we can reduce the laser-waveguide distance by a better well etching we will increase the total power coupled in the waveguide (slab+ridge) and at the same time the fraction which is coupled in the ridge increases.

The laser-waveguide coupling efficiency at the start of the thermocompression process differs with the value at the end. see Fig.3. We observe difference in the order of $\pm 25\%$. The most likely cause of these changes is a change in the alignment.

#### 4.4.2. Thermal characteristics

We have also investigated the thermal stability of the laser-waveguide coupling. For this purpose we have recorded current-power curves as function of substrate temperature. In the left part of Fig.4 we have plotted for $I_{forward} = 50$

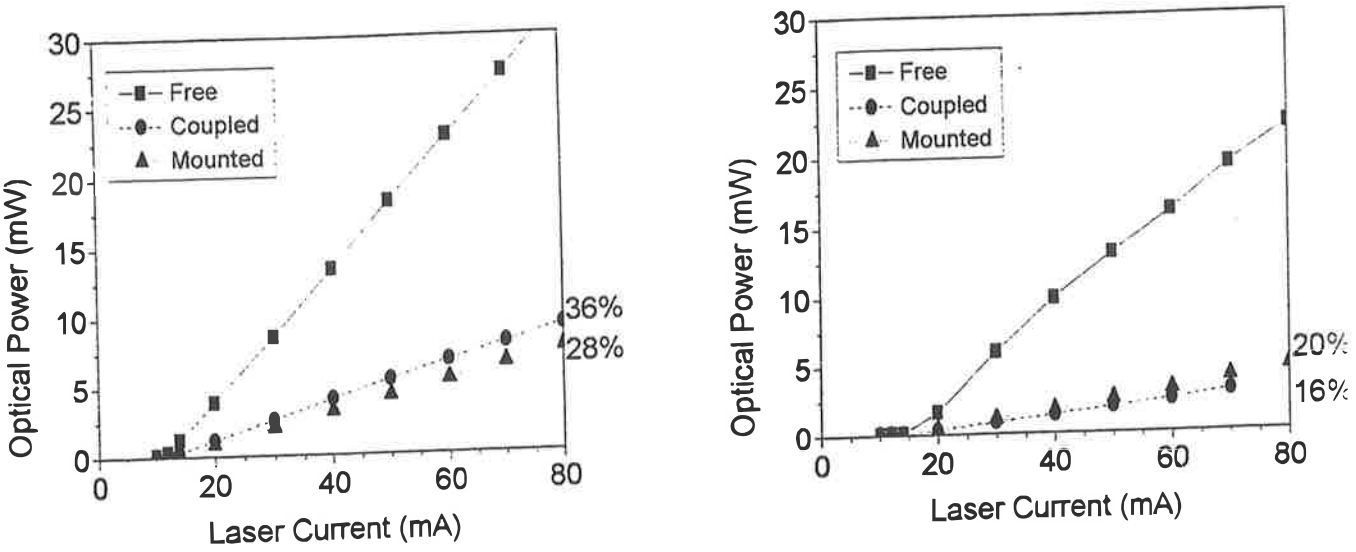


**Figure 3.** Measured laser-waveguide coupling efficiency. (Left) coupling of a 850 nm laser to SiON waveguide. (Right) coupling of a 850 nm laser to a $Si_3N_4$ ridge waveguide

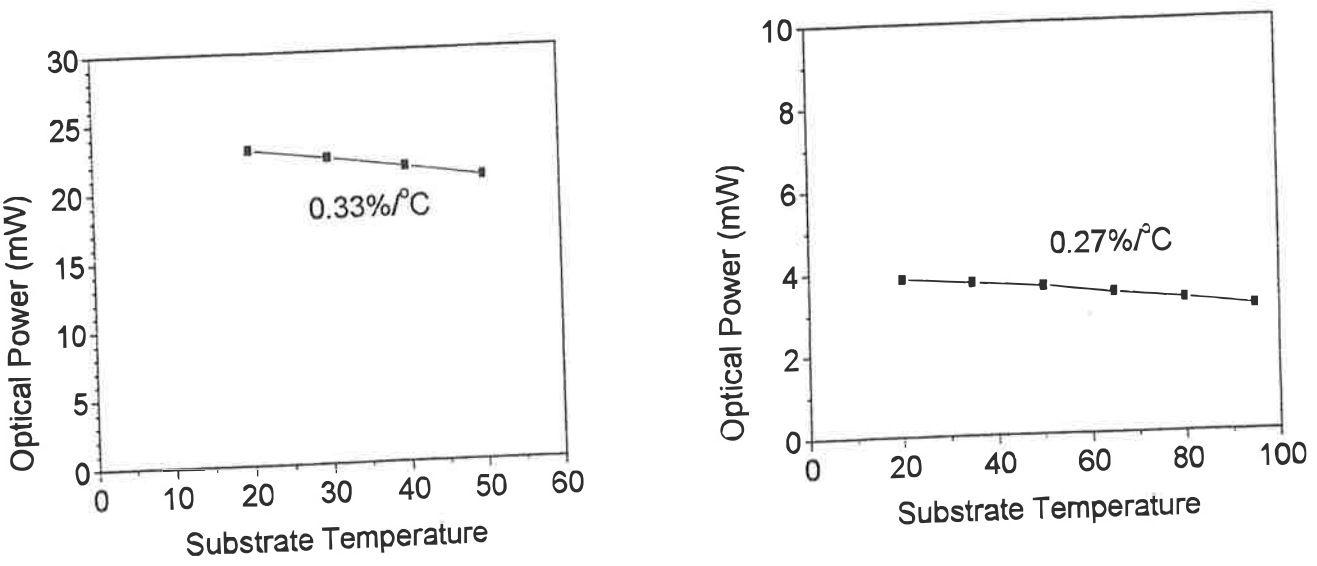


**Figure 4.** Temperature sensitivity. (Left) A bare 850 nm laser and (right) a coupled laser to a SiON slab waveguide

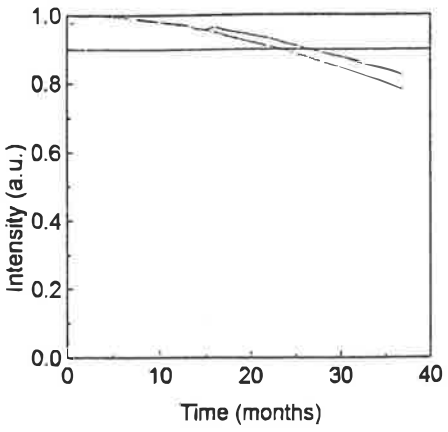


**Figure 5.** Degeneration curve of 850 nm lasers

mA CW (continuous wave, duty cycle 100%) the emitted optical power for a bare 850 nm diode laser as function of the substrate temperature. The temperature sensitivity is found to be -0.33%/°C. On the right side of the same figure we have repeated the experiment for a laserdiode coupled with thermocompression to a slab SiON waveguide. In this case a duty cycle of 5% was used. As can be seen the thermal characteristics of the coupled laserdiode is almost unaltered (-0.27%/°C). This means that the thermocompression bond is thus thermally stable.

### 4.5. Lifetime of mounted laserdiodes

The induced lifetime reduction of laserdiodes is among others dependent on the pressure the lasers experience during the handling/mounting process. The yield strength of GaAs is about $10^4$ bar. Dislocations become mobile at a pressure of a few times $10^3$ bar. During electron-hole recombination processes within the GaAs crystal dislocations become already mobile at $10^2$ bar.[18] When this happens a fast degeneration of the laser can result. Goodwin *et al.*[19] found that the pressure also influences the slow laser degeneration. He found a correlation between the low degeneration speed and the maximum pressure the laser experienced during handling. Goodwin advised to keep the pressure in the active region of an $Ga_{1-x}Al_xAs$ laser below 100 bar. So we are in the danger zone with our bonding pressure and it is essential to test the lifetime of thermocompression bonded laserdiodes.

The laserdiodes were tested at constant current mode at elevated temperatures. There was no burn-in pre-screening. The laserdiodes were mounted epi-down at the edge of metallized silicon substrates. The output power is monitored by silicon photodiode just in front of the laserdiode. Before and after laser mounting and also after wire-bonding the current-power curves of the laserdiodes were recorded and compared.

In the present study the lasers were not mounted in front of waveguides. However it is also relevant to test the lifetime of lasers coupled to $Si_3N_4$ ridge waveguides. The additional manipulation of the lasers needed for optimization of the coupling efficiency can introduce crystal defects in the laser crystal which can grow/move into the active layer and thus increase the degeneration rate. (Note that this type of accelerated degeneration is common for most of the hybrid waveguide coupling techniques as described in section 2).

The gradual degradation of the laserdiodes as shown in Figs.5,6 is thermally activated. The degeneration rate $R$ is described by: $R = R_0 exp(-E_a/k_bT)$, where the activation energy $E_a$ can be in the range $0.6 - 1$ eV for AlGaAs (850 nm) lasers.[20] For the AlGaInP lasers an activation energy of 0.8 eV[21] and 1.0 eV[22] is reported. So degeneration can be speeded up by testing the lifetime of the laserdiodes at elevated temperatures (acceleration factor: $exp(-\frac{E_a}{k_b}(\frac{1}{T_2} - \frac{1}{T_1}))$).

#### 4.5.1. 850 nm lasers

Two 850 nm laserdiodes are tested CW at a forward current of 29.5 mA at a temperature of 50°C at an initial output power of 9 mW. After 3 years their output intensity as monitored with a silicon photodiode has dropped to about 79%. Assuming an application in which the failure criterion is set at 10% reduction in output power than the lasers

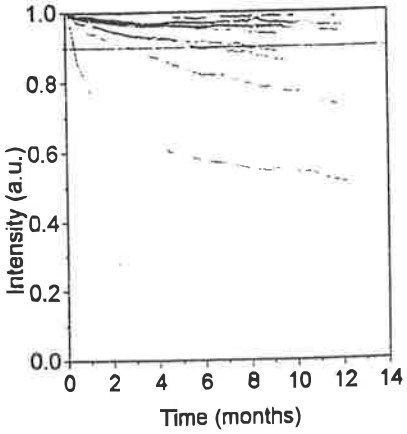


**Figure 6.** Degeneration curve of 675 nm lasers

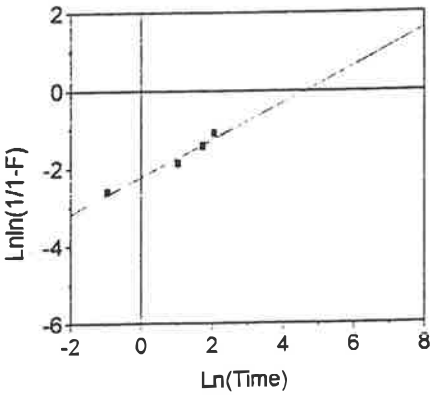


**Figure 7.** Weibull plot of degenerated 675 nm lasers

survived for 24 and 27 months as can be seen in Fig.5. Estimating a defect motion activation energy of 1 eV, the estimated lifetime at 30°C will be 21 and 24 year respectively.

### 4.5.2. 675 nm lasers

The 675 nm laserdiodes are tested CW at a forward current of 50 mA. Since the 675 nm laserdiodes are far more temperature dependent than the 850 nm laserdiodes we have lowered the testing temperature to 40°C. The initial output power at 40°C was 7-9 mW. To determine the mean time to failure (MTTF) of this laserdiode type we simultaneously tested 13 lasers out of the same laser badge. One of the lasers showed some saturation in optical power versus forward current ($I_{forward} > 60$ mA) at the start of the test. This laser was also the fastest degenerating laser. Its output power dropped below 10% in 0.4 months. Three other lasers have also dropped in intensity below 10% (after 2.8, 5.7 and 7.8 months) while the rest of the lasers are still operating after 9.5 - 12 months, as can be seen in Fig.6. With the same failure criterion and defect activation energy as used above, the estimated lifetime at 30°C for the degenerated lasers is 1.3, 9.7, 19.3, and 26.7 months, for the remaining lasers the estimated lifetime will be longer than 32-41 months.

### 4.5.3. Analysis and discussion

Due to the larger number of tested 675 nm lasers a statistical failure analysis can be made for these types of lasers. At present the number of failed lasers is insufficient for an accurate analysis though. Normal degeneration curves can be divided into three regions: (1) burn-in period in which production failures show up ; (2) random failure period;

(3) wear-out period in which devices come to their operational life. For each region a statistical failure distribution function can be used. A very convenient and appropriate failure distribution function in case of degeneration of electro-optic components is the Weibull distribution function. This function can be used for all three degeneration regions. The Weibull failure distribution function $F(t)$, which give the fraction of failed components is given by the following equation[23]:

$$F(t) = 1 - exp\{-[(t-\gamma)/\eta]^m\} \tag{1}$$

with $t$ the time. $m$ the shape parameter describing the region in the general degeneration curve (m = 1 constant failure rate due to random failure), $\eta$ the scale parameter, $\gamma$ location parameter ($\gamma = 0$ if failure is considered just after starting the test as we did). The MTTF is given by MTTF $= \eta\Gamma(1+1/\mathrm{m})$. The analysis of Fig.7 gives a shape parameter of 0.48. This indicates that we have a combination of initial failure and constant failure. For the 675 nm lasers operated in constant current mode at a forward current of 50 mA (7-9 mW) at a temperature of 30°C we determined a MTTF of 30 year (assuming a defect activation energy of 1 eV). The error margins are however large due to the low number of degenerated lasers.

All tested lasers show a gradual degeneration related to point-defects. No sudden failures due to growing dark line defects have appeared. Dark line defects starts to grow at dislocations in the laser crystal (introduced during handling or crystal growth) under influence of e-h recombination. When they reach the active region a sudden failure occurs. The absence of sudden failures indicates in case of the 850 nm lasers that the pressure used in the thermocompression process is not creating dislocations. An increased gradual degeneration can than possibly be related to residual stresses present in the laser crystal after mounting. In case of the 675 nm lasers no such conclusion can be reached, since it is reported that the presence of indium in the laser material prevents the growth of dark line defects due to dislocation pinning.[24]

It therefore seems that the influence of the thermocompression process on the degeneration rate of the lasers is modest. The thermocompression method is thus a very attractive technique to couple a wide variety of laserdiodes to a wide variety of waveguides. This also means that the laser bonding technique is very suitable for the sensor applications we have in mind.

## 5. BASIC SENSOR CIRCUIT

The main application area we have in mind for our coupling technique is related to chemical and physical sensors. In a combined project with the University of Twente we have developed a hybrid electro-optic sensor platform. This sensor platform combines most of the hybridizations developed in the joint project. We recognize in Fig.8 the hybrid laser-waveguide coupling and a hybrid photodiode-waveguide coupling.[25] In the basic platform the optical waveguide circuitry are still very simple. It consists of straight ridge $Si_3N_4$ waveguides. Also electronic chips for laserdriving and amplifying/buffering the photodetector signal is noticable. The sensor platform is now in its most principal form ready for realizing very compact optical micro sensors.

## 6. CONCLUSIONS

A reliable high-precision laser coupling method has been demonstrated. The coupling method is very versatile since it is independent of laserdiode type and waveguide structure. The thermocompression mounting process has only a moderate influence on the laserdiode lifetime. Apart from sensor applications on which we are presently concentrating other application areas are within reach, like e.g. integrated erbium-doped waveguide amplifiers (here we can apply our coupling technique to couple the pump laser to the doped waveguide) or blue-laser light generation (also for coupling the pump laser but now to the non-linear waveguide).

To demonstrate the viability of the laser-waveguide coupling concept, a general platform for integrated opto-electronic sensor systems on silicon has been realized. The system has been build upon silicon substrate and incorporates a hybridly integrated semiconductor laser, photodetector, electronics and $Si_3N_4$ optical waveguides.

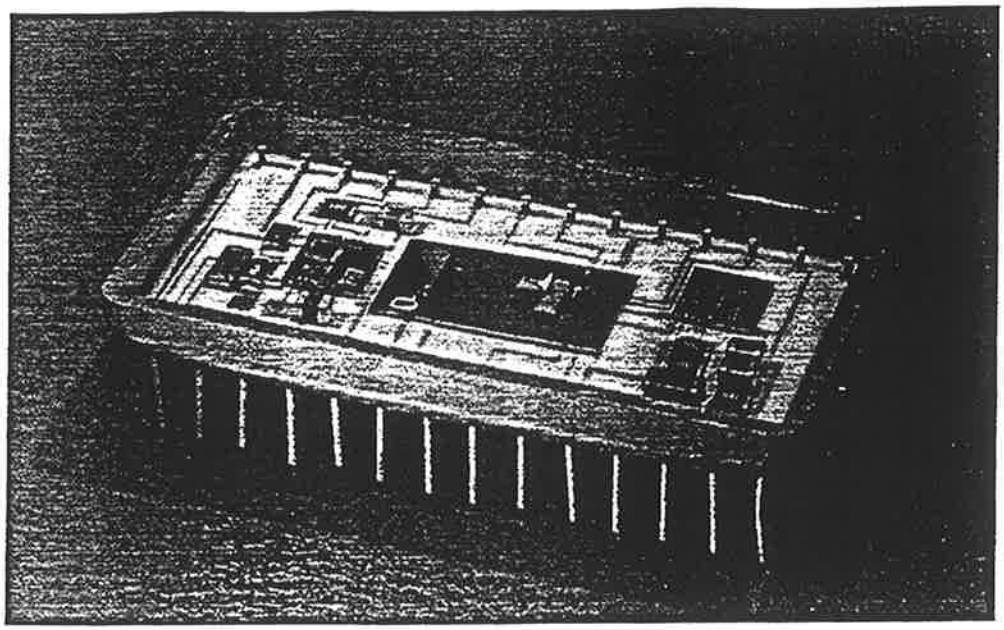

**Figure 8.** Basic sensor platform with hybridly coupled laser

## ACKNOWLEDGEMENTS

The authors wish to thank their colleagues K.W. Benoist, J.A.G. van Bezooijen, J.L. Joppe, R. Verboom for fruitfull discussions and support. SiON and $Si_3N_4$ based waveguides were made available by the group of Paul Lambeck of the University of Twente. This work was in part financially supported by the Royal Dutch Navy and IC Technology Program (IOP Electro-Optics) of the Dutch Ministry of Economic Affairs.

## REFERENCES

1. K. Mizuishi, "Some aspects of bonding-solder deterioration observed in long-lived semiconductor lasers: Solder migration and whisker growth," *J. Appl. Phys.* **55**, pp. 289–295, 1984.
2. M. Fukuda, O. Fujita, and G. Iwane, "Failure modes of InGaAsP/InP lasers due to adhesives," *IEEE CHMT* **7**, pp. 202–206, 1984.
3. Y. Yamada, H. Terui, Y. Ohmori, M. Yamada, A. Himeno, and M. Kobayashi, "Hybrid-integrated 4 x 4 optical gate matrix switch using silica-based optical waveguides and LD array chips," *IEEE LT* **10**, pp. 383–390, 1992.
4. E. Friedrich, M.G. Öberg, B. Broberg, S. Nilsson, and S. Valette, "Hybrid integration of semiconductor lasers with Si-based single-mode ridge waveguides," *IEEE LT* **10**, pp. 336–339, 1992.
5. L. Goldmann, "Geometric optimization of controlled collapse interconnections," *IBM J. Res. Develop.* **13**, 1969.
6. M. Wale and C. Edge, "Self-aligned flip-chip assembly of photonic devices with electrical and optical connections," *IEEE CHMT* **13**, pp. 780–786, 1990.
7. Y. Yamada, F. Hanawa, T. Kitoh, and T. Maruno, "Low-loss and stable fiber-to-waveguide connection utilizing UV curable adhesive," *IEEE PTL* **4**, pp. 906–908, 1992.

8. P. Demeester, I. Pollentier, P. de Dobbelaere, C. Brys, and P. van Dale, "Epitaxial lift-off and its applications," *Semicond. Sci. Technol.* **8**, pp. 1124–1135, 1993.
9. R. Berry, P. Hall, and M. Harris, *Thin film technology*, Van Nostrand Reinhold Company, New York, 1968.
10. A. Hill and E. Wallach, "Modelling solid-state diffusion bonding," *Acta Metall.* **37**, pp. 2425–2437, 1989.
11. J. Jellison, "Kinetics of thermocompression bonding to organic contaminated gold surfaces," *Proc. Electronic Components Conf.* , 1976.
12. J. Jellison, "Effect of surface contamination on the thermocompression bondability of gold," *IEEE PHP* **11**, p. 206, 1975.
13. T. Enjyo, K. Ikeuchi, and N. Akikawa, "Effect of the roughness of faying surface on the early process of diffusion welding - study of the early process of diffusion welding by means of electric resistance measurement (report 2)," *Trans. JWRI* **11**, p. 49, 1982.
14. L. Maissel and R. Glang, eds., *Handbook of thin-film technology*, McGraw-Hill, New York, 1970.
15. J. Joppe, A. de Krijger, and O. Noordman, "Hybrid integration of laser diode and monomode high contrast slab waveguide on silicon," *Electron. Lett.* **27**, p. 162, 1991.
16. H. Albers, L. Hilderink, J. Berends, K. Wörhoff, N. van Hulst, and P. Lambeck, "A waveguide material for integrated optical sensors: silicon oxynitride," *Proc. 1996 National Sensor Conference* , pp. 221–230, 1996.
17. K. Wörhoff, P. Lambeck, H. Albers, N. van Hulst, and T. Popma, "Optimisation of LPCVD silicon oxynitride growth to large refractive index homogeneity and layer thickness uniformity," *European Symposium on Lasers and Optics in Manufacturing* , 1997. This proceedings.
18. T. Kamejima, K. Ishida, and J. Matsui, "Injection-enhanced dislocation glide under uniaxial stress in GaAs-(GaAl)As double heterostructure laser," *Jap. J. Appl. Phys.* **16**, p. 233, 1977.
19. A. Goodwin, P. Kirkby, I. Davies, and R. Baulcomb, "The effect of processing stresses on residual degradation in long-lived $Ga_{1-x}Al_xAs$ lasers," *Appl. Phys. Lett.* **34**, p. 647, 1979.
20. R. Waters, "Diode laser degradation mechanisms: a review," *Prog. Quant. Electr.* **15**, pp. 153–174, 1991.
21. K. Endo, K. Kobayashi, H. Fujii, and Y. Ueno, "Accelerated aging for AlGaInP visible laser diodes," *Appl. Phys. Lett.* **64**, pp. 146–148, 1994.
22. Philips Opto-Electronics Centre, *Shortwavelength semiconductor lasers brochure*, 1994. Preliminary specification data sheets.
23. M. Fukuda, *Reliability and degradation of semiconductor lasers and leds*, Artech House, 685 Canton Street Norwood, MA 02062, 1991.
24. S. Yellen, A. Shepard, R. Dalby, J. Baumann, H. Serreze, T. Guido, R. Soltz, K. Bystrom, C. Harding, and R. Waters, "Reliability of GaAs-based semiconductor diode lasers: 0.6-1.1 $\mu$m," *IEEE QE* **29**, pp. 2058–2067 1993.
25. A. de Krijger and H. Bekman 1997. to be published.

PROCEEDINGS OF SPIE
EUROPTO SERIES

# Micro-optical Technologies for Measurement, Sensors, and Microsystems II
and
# Optical Fiber Sensor Technologies and Applications

**Olivier M. Parriaux**
**Ernst-Bernhard Kley**
**Brian Culshaw**
**Magnus Breidne**
*Chairs/Editors*

**18–20 June 1997**
**Munich, FRG**

*Sponsored by*
EOS—The European Optical Society
SPIE—The International Society for Optical Engineering
The Commission of the European Communities, Directorate General for Science, Research, and Development


**Volume 3099**